Analytica Chimica Acta 1047 (2019) 115–123

Contents lists available at ScienceDirect

Analytica Chimica Acta

journal homepage: www.elsevier.com/locate/aca

High-throughput deposition of chemical reagents via pen-plotting technique for microfluidic paper-based analytical devices

Mohammad Rahbar [a], Pavel N. Nesterenko [a], Brett Paull [a], Mirek Macka [a, b, c, *]

[a] Australian Centre for Research on Separation Science (ACROSS), School of Natural Sciences, University of Tasmania, Hobart, 7001, Australia
[b] Department of Chemistry and Biochemistry, Mendel University in Brno, Zemedelska 1, CZ-613 00, Brno, Czech Republic
[c] Central European Institute of Technology, Brno University of Technology, Purkynova 123, CZ-612 00, Brno, Czech Republic

HIGHLIGHTS

- A pen-plotting technique is characterized for chemical ink deposition on μPADs.
- A gravimetric approach is introduced to measure the deposition volume.
- Deposition is studied for different geometrical forms (circular and linear).
- The effect of plotting parameters on deposition is investigated.
- The approach is demonstrated by a fluorescence-based determination of Al in waters.

GRAPHICAL ABSTRACT

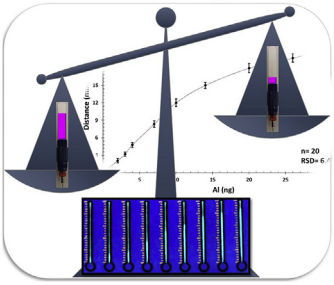

ARTICLE INFO

Article history:
Received 8 June 2018
Accepted 4 September 2018
Available online 6 September 2018

Keywords:
Microfluidic paper-based analytical device
Reagent deposition
Technical pen
Plotter
Distance-based detection
Aluminium determination

ABSTRACT

The deposition of chemical reagent inks on paper is a crucial step in the development and fabrication of microfluidic paper-based analytical devices (μPADs). A pen-plotting approach, delivering chemical ink deposition using technical pens filled with reagents and inserted into a desktop electronic plotter, is shown herein to be a versatile, low-cost, simple, rapid, reproducible, and high-throughput solution. The volume of the deposited ink was quantified gravimetrically, confirming that nanoliter volumes of reagents can be deposited reproducibly (e.g. 7.55 ± 0.37 nL/mm for a plotting speed of 10 cm/s) in detection zones of μPADs, typically spatially defined using wax printing. This approach was further investigated with regard to deposition of reagents in different geometrical forms (circular and linear), so demonstrating its applicability for preparation of μPADs with flexible design and application. By adjusting the plotting speed for linear deposition, lines with a relatively large range of widths (≈628–1192 μm) were created. Circular deposition was also demonstrated via delivery of reagents within wax printed circular fluidic barriers of a range of diameters (inner diameter = 1.5–7 mm). These capabilities were practically demonstrated via the fabrication of μPADs, based upon differing detection principles for determination of aluminum in natural waters using Morin as the fluorescent reagent. Traditional μPADs based on digital image colorimetry (DIC) were produced using circular deposition, whilst distance-based μPADs exploited linear deposition. Both types of μPADs developed using this method showed excellent precision for determination of trace concentrations of aluminium (average RSDs = 3.38% and 6.45%, and LODs = 0.5 ng (0.25 ppm) and 2 ng (0.5 ppm), for traditional and distance-based detection, respectively).

* Corresponding author. Australian Centre for Research on Separation Science (ACROSS), School of Natural Sciences, University of Tasmania, Hobart, 7001, Australia.
E-mail addresses: Mirek.macka@utas.edu.au, miroslav.macka@ceitec.vutbr.cz (M. Macka).

https://doi.org/10.1016/j.aca.2018.09.006

1. Introduction

In the last decade, there has been significant interest in the development of microfluidic paper-based analytical devices (μPADs) in order to meet the increasing demands of low-cost, rapid, portable, and disposable technologies, in the fields of environmental, biomedical and industrial analysis [1–3]. μPADs are easy-to-use miniaturized analytical devices, which are fabricated by creating fluidic barriers defining confined hydrophilic areas on a paper substrate, using wax printing or another related technique [4,5]. The fabrication process then involves the deposition of chemical reagents (e.g. colorimetric reagents, buffers, conductive inks, etc. depending on the detection principles and applications) upon the paper [6–8].

Obviously homogeneous and reproducible deposition of the reagents is a crucial element in μPAD preparation, especially in the case of distance-based μPADs, where the sample should have a uniform, reproducible and unrestricted flow through the microfluidic channels to react with the colorimetric reagents. Distance-based μPADs rely on measurement of the length of a color band formed on a straight microfluidic channel resulting from colorimetric reactions taking place between the analyte (present in the sample) and pre-deposited chemical reagents [9–14]. Even in traditional μPADs, which are based on color intensity measurements, having a homogenously deposited reagent leads to improved quantitative performance [15].

To-date this deposition step has been carried out using various methods, including manual pipetting, dipping, spraying, brushing, pneumatic dispensing, screen printing, photolithography, and inkjet printing. Each of these techniques has their inherent advantages and disadvantages, however some of them are more reliable and efficient than others. Inkjet printing has been shown to be one of the most successful approaches, providing deposition of reagents with high resolution and accuracy, and precise control over volumes of deposited material (picoliter-sized droplets) [16–22]. Inkjet printing does however suffer from tedious modification steps, and time-consuming print head and cartridge washing steps for different reagents. Additionally, inkjet printers can also be incompatible with certain biological reagents (e.g. inks containing proteins), as they either apply a heat pulse (thermal printers) or shear force (piezoelectric printers) to the corresponding inks [17].

Recently we reported upon the deposition of reagents using technical pens inserted into a low-cost electronic desktop plotter, as a simpler, quicker, more flexible, and also more convenient approach to μPAD formation [23]. The alignment of the plotting step with the wax printed microfluidic features, which was the main concern associated with the pen-plotting technique, was also addressed in a follow-up study [24]. The chemical reagents were deposited exactly in user-selected spots (detection zones defined via wax printing) on the paper by activating the optical scanner of the Cameo plotter/cutter, along with some other required commands.

Pen-plotting offers many advantages over the above techniques, including inkjet printing. With pen-plotting there is no need for modification and the pen cartridge can be easily and quickly ($\leq$3 min) opened, washed, dried and refilled with new reagents. It is also flexible in terms of substrate material, as plotting can be carried out with numerous substrates such as filter paper, nitrocellulose membranes, etc., and contrary to inkjet printers, pen-plotting is non-destructive, as no kind of pulse or force is applied to the reagents. The technical pens are also compatible with most organic solvents, which may be used in the formulation of the chemical reagent inks. Finally, they are also more flexible in terms of the viscosity of the reagent inks used, as a variety of inks can be plotted on paper without the need for viscosity modifiers, surfactants, etc.

However, in spite of all these advantages, currently there is still a high degree of uncertainty in terms of the ink deposition volume on the substrate using the pen-plotting technique. Also, apart from the very basic and simple linear deposition mode, the applicability of the pen-plotting approach for more complex designs and geometries has not yet been demonstrated. Therefore, in this work, we used an accurate gravimetric method to quantify the amount of deposited ink on paper as volume per length (nl/mm, for linear deposition) or per area (nl/mm^2, for circular deposition). The performance of the pen-plotting approach was also further characterized by investigating its coverage capability for ink deposition on μPADs with various shapes and designs (e.g. straight lines or circles). Further, the effect of plotting speed on the width of the plotted lines and the diameter of plotted circles was investigated. The versatility of the pen-plotting deposition approach was demonstrated via the determination of aluminum in natural water samples using μPADs based upon two different detection principles, specifically a traditional color intensity based analysis, and also a distance-based detection method. In this regard, a fluorescence-based determination of aluminum using a Morin complexing agent was performed on the surface of paper.

2. Experimental section

2.1. Chemicals and materials

All chemicals were of analytical reagent grade. Morin, acetic acid, sodium acetate, 1,10-phenanthroline, hydroxylamine hydrochloride, and rhodamine 6G, were purchased from Sigma-Aldrich. Standard solutions of Na(I), K(I), Pb(II), Ni(II), Zn(II), Mg(II), Mn(II), Ca(II), Co(II), Cd(II), Cr(II), Fe(II), Hg(II), Fe(III), and Al(III) metal ions were prepared in deionised water by diluting a stock solution of 1000 mg/L (in 5% nitric acid) of the nitrate salt of each element supplied by BDH Chemicals (Queensland, Australia). All the solutions were used immediately after preparation. Deionised water was obtained with a Millipore (Bedford, MA, USA) Milli-Q water purification system. Whatman grade 1 qualitative filter paper with a pore size of 11 μm and thickness of 180 μm (GE Healthcare Australia Pty. Ltd, NSW, Australia) was used to fabricate the μPADs. Transparent film (125 μm thickness, GBC®, NSW, Australia) was used to laminate the μPADs.

2.2. Instrumentation

A wax printer (Colorqube 8870, Xerox, Norwalk, CT, USA) was used to print the microfluidic designs on the filter paper. A desktop electronic craft plotter/cutter (Silhouette CAMEO®, Kuluin, QLD, Australia) was used to deposit chemical inks on the detection zones of the μPADs. The deposition was performed using Mars®matic 700 technical pens (STAEDTLER Mars GmbH & Co. KG, Nuernberg, Germany, line width = 0.5 mm) filled with the desired reagents and inserted into the pen holder of the Cameo plotter. We have previously reported that these pens are compatible with most organic solvents [23]. Silhouette Studio® (V4.1.156) free software was used to design the desired patterns for both characterization experiments and also fabrication of μPADs. A Silhouette Cameo reusable cutting mat (12″ × 12″ Cut12) was used for the precise loading of the paper media into the plotter. An A3 laminator (LM330, Laminating Wholesalers, VIC, Australia) with adjustable lamination temperature was used to laminate the devices from the bottom side to prevent any possible leakage of solutions. A Dino-Lite EDGE digital fluorescence microscope (AM4115T-GFBW, SCINET, WA, Australia) with a magnification range of 20x-220x, controlled by DinoCapture 2.0 free software, was used for all required optical

measurements. The digital image colorimetry (DIC) experiments were also accomplished by the same microscope and corresponding software. A UV viewing cabinet (Spectroline®, CM-10, NY, USA, UV light source = 254 nm) was used for observation of the fluorescence emission from the Al-Morin complex developed over the straight microfluidic channels of the distance-based μPADs. A Nikon digital DSLR camera (D90 with AF-S DX NIKKOR lens, Nikon Australia Pty Ltd) was used to capture the photographs of the distance-based μPADs after fluorescence emission under UV illumination. A Sartorius analytical balance (MC 210 S, readability: 0.01 mg) was used for all gravimetric measurements.

2.3. Design and fabrication of μPADs

The overall fabrication process of μPADs is depicted in Fig. S1. The required microfluidic designs (Fig. S2) for both traditional and distance-based μPADs were produced using the free Silhouette Studio® software and printed on both sides of the paper using the wax printer. The "Registration Marks" option in the software was also selected prior to printing to ensure alignment of the printed feature with the following deposition step [24]. As depicted in Fig. S2, the distance-based pattern (designed line width = 0.4 mm before wax melting) was composed of a circular sample zone (3.5 mm diameter) and a straight channel (1.2 × 25 mm) along with some scale bars, which were drawn at 1 mm intervals next to the channel for direct measurement of the colored band length. The scale bars were intentionally chosen to be red in color for clear identification of the band length when the μPADs were placed in the dark UV viewing cabinet required for the determination of aluminum (the red gave the highest contrast of the ten available colors). The sizes of both the sample zone and the channels were optimized for storage of the lowest possible volume of sample (4 μL), while at the same time having a stable fluid flow and obvious color change. The traditional μPADs were comprised of simple circles with diameter of 3.4 mm and designed line width of 0.5 mm (before wax melting). In the next step, the technical pens were filled with the corresponding chemical reagents and then inserted into the plotter to deposit the reagents on the detection zones. Afterward, the sheet was laminated (165 °C) from the bottom side in order to melt the wax through the thickness of the paper and also to give a higher mechanical stability to the fabricated μPADs and preventing any fluid leakage during analysis. While laminating, the top side of the device was covered with a piece of copy paper to avoid contamination of the laminator rollers with the melted wax and also to limit overexposure of the printed features to heat.

2.4. Gravimetric analysis

Fig. 1A shows a flow chart depicting the gravimetric approach proposed in this work to measure deposition volumes. First, a certain volume (1 mL taken by a micropipette) of the model chemical ink (rhodamine 6G, 0.1% w/v in water-ethanol mixture 50% v/v) was weighed (n = 10) using the analytical balance, to obtain the density of the ink. Then, the pen cartridge was filled with the ink, attached to the nib body, and shaken a few times to help the ink to reach the tip. Considering the working principles of technical pens (described in Supporting Information), the tip was drawn along the paper to trigger the ink flow. After that, the filled pen (excluding the pen holder) was weighed and the initial mass was recorded. To keep potential weighing errors to a minimum, the pen holder was not included in the gravimetric measurements since it is not engaged in the ink delivery process so does not need to be weighed, whilst all the other components of the pen (Fig. S3) were in contact with the ink so required weighing. After obtaining the initial mass, the pen was inserted into the plotter and a large number (N = 400) of straight lines (30 mm length) were plotted on a sheet of filter paper (A4 size) to simulate a number of individual linear depositions. Next, the pen holder was detached and the remainder reweighed to determine the final mass. The difference between the two measurements was equal to the consumed mass of ink (e.g. 0.14281 ± 0.00213 g for plotting speed = 5) under the given conditions. Subsequently the mass of consumed ink for each individual plotted line and every millimetre (mm) of each line was obtained through dividing the obtained total mass by the number of plotted lines (N = 400) and the length of each line (30 mm), respectively. This mass could then be converted to a volume (nL) by considering the measured density (0.88764 ± 0.00167 g) of the corresponding ink. Both the initial (e.g 5.84801 g) and final (e.g 5.70681 g) measured masses of the pen used for the gravimetric calculations, are very large numbers relative to the inherent error of the balance (0.01 mg). Therefore, the final calculated volume (nL) is reliable in terms of possible deviations resulting from weighing errors. The same procedure can be applied for circular deposition by plotting circles instead of lines and the deposition volume can be measured per unit of square millimetre (mm^2) of the paper. In this work, this was only performed with Morin solution as the chemical ink in order to quantify the deposition volume for color intensity based μPADs in the determination of Al(III).

2.5. Aluminum detection

The determination of Al(III) was based on the formation of a fluorescent coordination complex of this metal with Morin in a slightly acidic medium, resulting in an instantaneous color change [25–28]. Under UV radiation, Al gives an intense green fluorescence in reaction with Morin. The fluorescence-based reagent was prepared by mixing equal parts (%v/v) of acetate buffer solution (pH = 4, 0.2 M) with Morin solution (0.1% w/v in ethanol 50%). Then the reagent was deposited over the detection zones of the μPADs using the pen-plotting approach (constant plotting speed = 4 cm/s) and allowed to dry (5 min) for further analysis.

3. Results and discussion

We have previously shown how the pen-plotting approach can be a viable method for deposition of chemical reagent inks on paper for development of μPADs. However, there were some additional challenges with this technique, such as the precise positioning of deposition on desired user selected spots. This issue was resolved using the optical scanning function of the plotter [24]. An existing challenge with the pen-plotting approach is the uncertainty associated with the volume of the deposited ink on the substrate and the inability to predict the deposited volume. In the present work, we resolved this issue by implementing an elegant gravimetric approach to measure the volume of deposited ink on the paper. This is very significant as it provides practical quantitative information about the volume of deposited reagents which can be then used when developing and optimizing new assays on paper or other media.

3.1. Gravimetric quantification of deposition volume

It is worthwhile mentioning that among all conventional automatic deposition techniques, only automatic dispensers (usually used for development of lateral flow immunoassays) can deposit a known volume of ink (μL/cm) upon a substrate [29]. However, these come at a considerable expense, require regular maintenance (e.g. unclogging and cleaning steps), and can deliver misalignment of ink deposition with wax printed features, etc. With inkjet printing, as the most reliable deposition technique for μPADs, the maximum

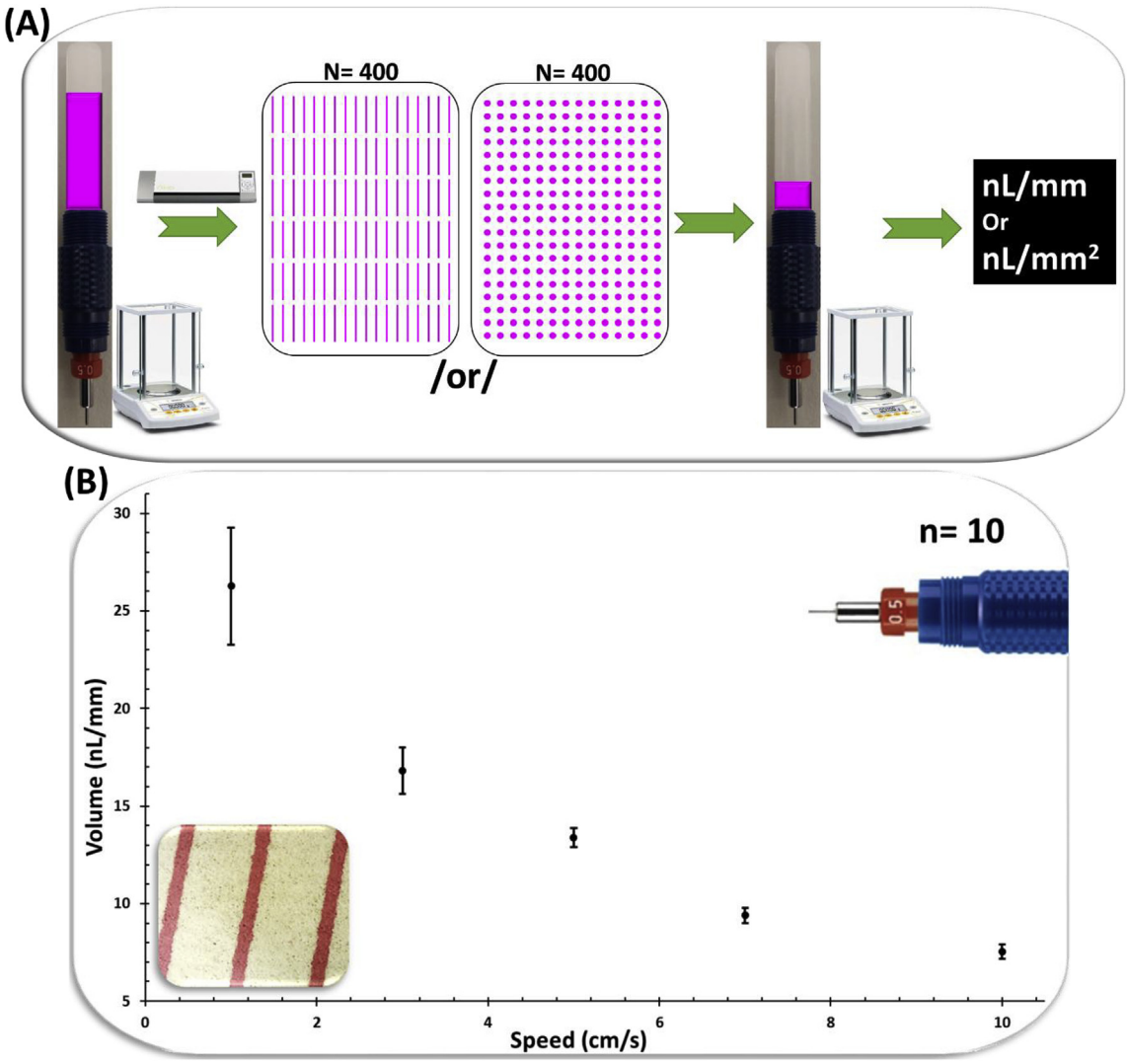

Fig. 1. (A) Flow chart of the gravimetric approach used for the determination of deposition volume. N is the number of corresponding plotted patterns (lines or circles). (B) Graph obtained from performing the gravimetric approach in the linear manner (n = 10) with varying plotting speeds (cm/s). The higher the speed, the lower the deposition volume (nL/mm). Inset: photograph of the plotted straight lines.

ejected volume can only be estimated from the printer features via mathematical calculations [30].

The gravimetric approach taken here is based on measuring the amount (mg) of ink consumed whilst plotting a large number of patterns (lines or circles) on the paper and then dividing the mass by that number to obtain the volume consumed for each individual pattern. The effect of plotting speed on the deposited volume was also investigated and the results were compiled as a graph (volume versus plotting speed) depicted in Fig. 1B. As anticipated, the higher the speed, the less the deposition volume per unit of length. The error bars indicate the standard deviations, which are higher for lower speeds (e.g. ±3.01 and ± 1.20 nL/mm for the speed of 1 and 3 cm/s, respectively); however, for medium and high speeds (e.g. 5 cm/s and higher) the errors are lower and almost the same (≈±0.41 nL/mm) showing the high reproducibility of the pen-plotting approach for reagent deposition. These small errors also confirm that the proposed gravimetric approach is a reliable method to determine the deposition volume. In addition, these results demonstrate how small volumes of reagent, as low as 7.55 ± 0.37 nL/mm (with plotting speed of 10 cm/s), can be precisely deposited on paper, which is sufficient to perform an assay without any need for multi-pass printing (as is usually required in inkjet printing to deposit sufficient reagents to produce strong signals [30]). However, it should also be noted that the numerical results presented here are for deposition of this particular model ink (rhodamine 6G, 0.1% w/v in ethanol 50% v/v), and will of course vary slightly for other inks of different viscosity and surface tension.

3.2. Full coverage of the detection zones

3.2.1. Linear deposition

We have already demonstrated linear deposition of colorimetric reagents inside wax printed microfluidic channels in the form of very simple straight lines, which were then used within μPADs with distance-based detection [24]. Here the linear deposition is further characterized and the effect of plotting speed on the width of plotted lines is investigated. This allows optimization of the plotting parameter settings for any particular application with specific device geometries. Technical pens were filled with the model ink (rhodamine 6G, 0.1% w/v in ethanol 50% v/v) and then straight lines (25 mm length) were plotted on the paper with different plotting speeds. Line width was measured by the fluorescence microscope

at five points along the lines (at increments of 4 mm) and the results are shown in the graph in Fig. 2. As expected, the higher the speed, the narrower the plotted lines, which signifies lower deposition volumes. This is also in agreement with the gravimetric measurements. These results indicate that by adjusting the plotting speed we can govern the width of the plotted lines across a relatively wide range of widths (≈628–1192 μm), which can be utilized later in the development of optimized μPADs designs. For instance, with this available line range, one single pass is enough to provide full coverage of a narrow detection zone, even for the narrowest reported wax printed channel used for distance-based measurements of ca. 900 μm [31]. For wider channels, the use of either lower plotting speeds or multiple linear deposition lines would be sufficient to cover the detection areas. The effect of reagent concentration on the width of plotted lines was also investigated; however, it was observed that the concentration had no significant effect on line width and only increased the color intensity of the plotted lines (Fig. S5). Detailed information about the microscopic measurements with a digital microscope used in this work is provided in the Supporting Information (Fig. S6).

3.2.2. Circular deposition

To further illustrate the applicability of the pen-plotting approach for deposition of reagents, we demonstrated a circular deposition of the model ink. This shows the suitability of this approach not only for distance-based μPADs, but also for traditional μPADs which are based on measurement of the color intensity in detection zones that typically have a circular shape. Circles with various diameters (0.25–4 mm) were designed by the Silhouette Studio® software and then plotted to emulate reagent deposition in circular detection zones within μPADs. The outer diameter of the plotted circles was measured by a fluorescence microscope and results are presented as a graph charting the measured diameter (M.D.) versus designed diameter (Fig. 3A). Circle designs with diameter in the range of 0.25–2 mm resulted in fully filled plotted circles with diameters in the range of 2.44 ± 0.06 to 3.26 ± 0.09 mm, which is in the typical size range of detection zones used in traditional μPADs. Diameters larger than 2 mm produced circles with empty centers since the amount of deposited ink was not enough to fully cover that area via ink wicking with the aid of the capillary effect. Thus, in order to fully cover detection zones larger than 3.26 mm, multiple circular deposition lines (Fig. 3B,b) could be implemented. To further demonstrate the circular deposition, circles with different sizes (inner diameter, 1.5–7 mm) were wax printed on the paper simulating traditional μPADs and then the pen-plotting approach was successfully applied to fill the circles with the model ink (Fig. 3B). Based on the obtained graph and also considering the constant line width of the plotted circles (≈1 mm), the required number of multiple deposition lines with given diameters could be designed to fully cover the corresponding regions (Fig. 3B). In the case of the smallest wax printed circle (1.5 mm), a single deposition line (0.25 mm length) instead of a circle was used to ensure the deposition would take place inside the desired area. In this case, the pen tip makes a small semicircular trace (diameter ≈ 1 mm) which was the smallest possible trace created by this approach with this particular ink. These experiments are an illustration of the suitability of the pen-plotting approach for a wide variety of applications.

3.3. Determination of aluminum in natural waters

The association between aluminum toxicity and some neurotic diseases such as Alzheimers, Parkinsons and dialysis encephalopathy in humans has been well documented. Therefore, determination of low concentrations of aluminum in natural waters and other environmental samples is vitally important [32,33]. Currently, several conventional analytical techniques such as atomic absorption or emission, mass spectroscopic techniques, and electrochemical methods are used for determination of Al(III) in water samples. Despite their high sensitivity and precision, these

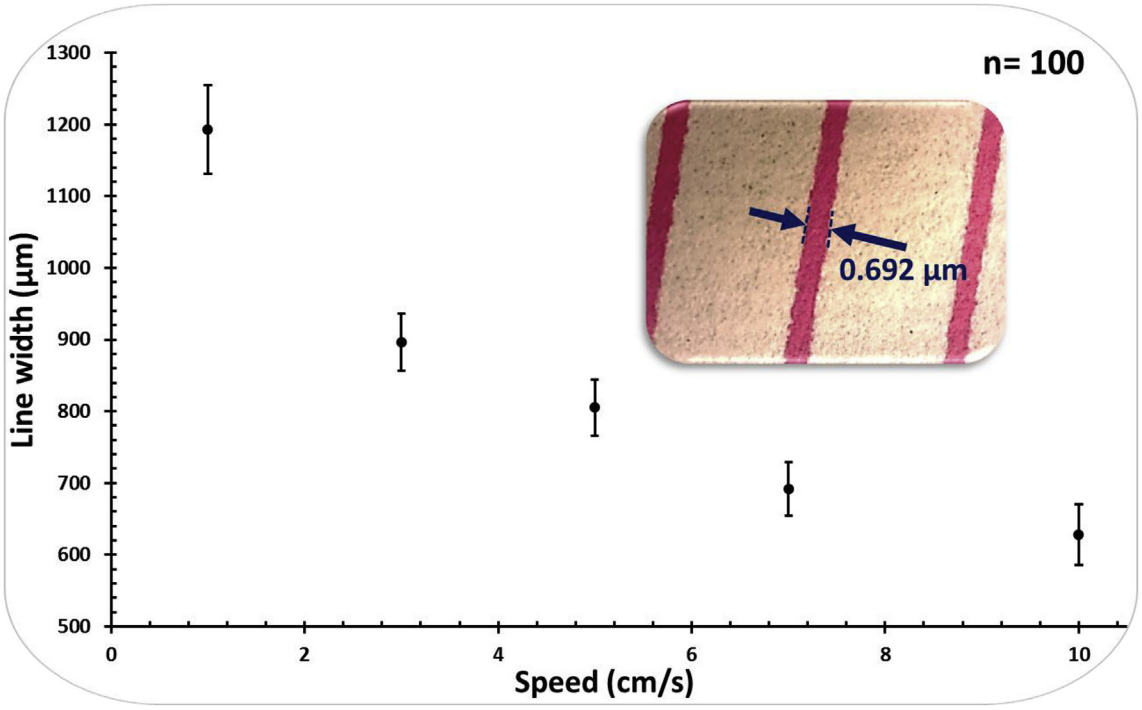

Fig. 2. Linear deposition and the effect of plotting speed (cm/s) on the width of plotted lines. The higher the speed, the narrower the plotted lines. Inset: photograph of the plotted lines. The error bars represent standard deviations from average values.

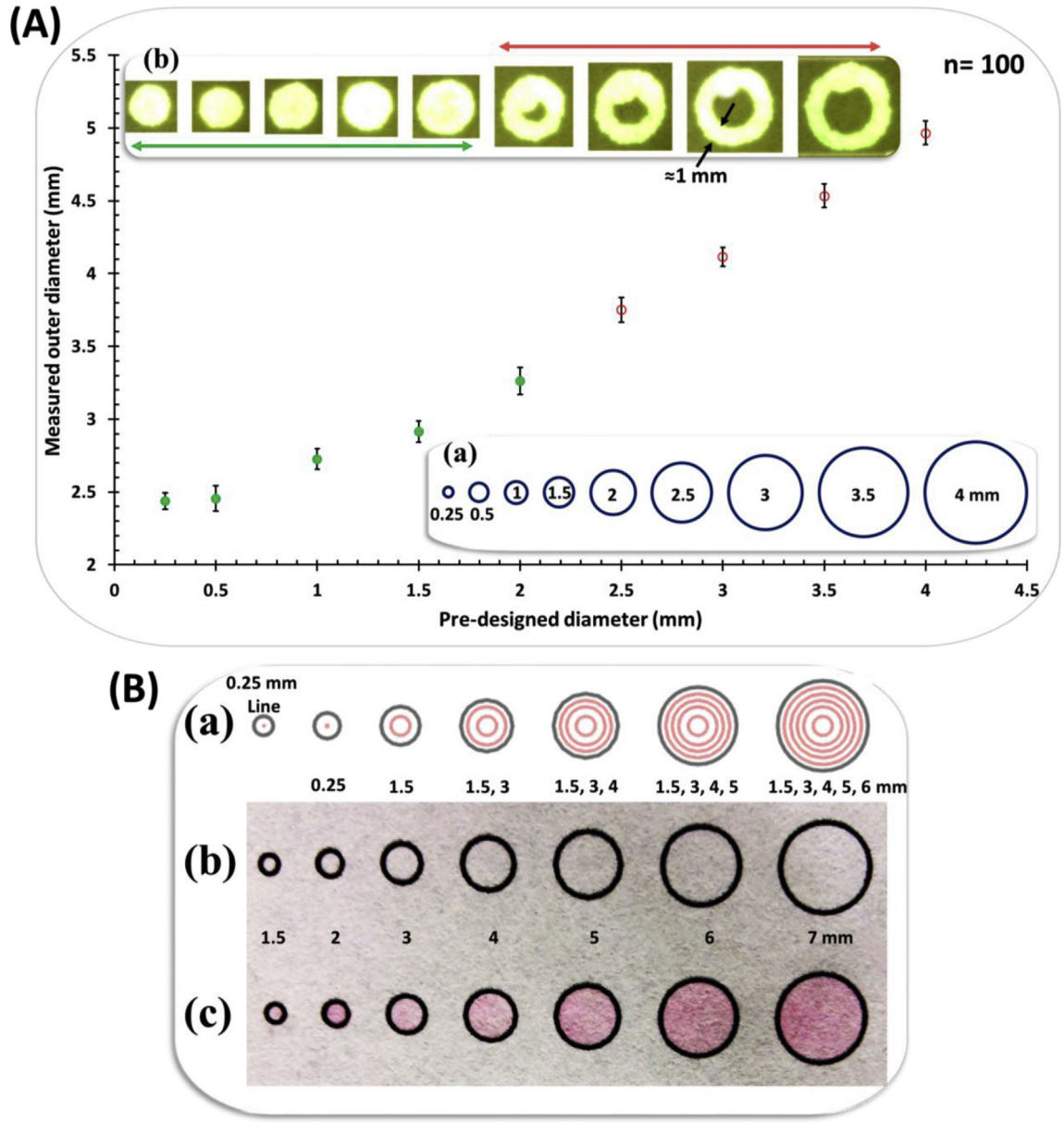

Fig. 3. Circular deposition. (A) Graph showing the relationship between diameters of designed circles (theoretical) vs. plotted circles (experimental, n = 100). Markers indicate fully filled (●) and unfilled (○) circles. Inset: (a) computer designed circles with various sizes. (b) photograph of the plotted circles. The unfilled circles had almost identical line widths (≈1 mm). (B) Demonstration of circular deposition to fill up wax printed circles with different sizes. (a) computer designed circular deposition lines (red circles) with their corresponding diameters. In order to fill up wax printed circles larger than 4 mm, multiple deposition lines (more than one deposition line) were used. (b) Photograph of wax printed circles with their corresponding diameters. (c) Photograph of wax printed circles after being filled up by performing the circular deposition. (For interpretation of the references to color in this figure legend, the reader is referred to the Web version of this article.)

methods are costly and time-consuming, and they need complex equipment and trained operators, which are all properties unsuitable for on-site analysis. Alternatively, μPADs can be utilized for rapid, low-cost, instrument-free, and portable analysis of the water samples.

To demonstrate the analytical potential of the technical concepts presented here, the fluorescence-based determination of aluminum was investigated using both distance-based and traditional μPADs. The gravimetrical approach was used (n = 4) to measure the deposition volume of the fluorescent reagent (Morin, 0.1% w/v in ethanol 50%) in various detection zones. Deposition volumes were 16.62 ± 0.38 nL/mm and 42.88 ± 2.15 nL/mm^2 for distance-based and traditional μPADs, respectively. Straight lines (line width = 748 ± 0.02 μm) and fully filled circles (outer diameter = 2.82 ± 0.07 mm) were used to cover the straight channel and circular shaped detection zones of the corresponding μPADs. The amount of reagent deposited in the detection zone was optimized (by changing the concentration) to create the best color contrast, along with the highest sensitivity on the μPADs.

3.3.1. Distance-based measurement

It is obvious that having reproducible linear deposition of the reagent over the detection channels in individual μPADs is essential for reproducibility and precision of the analysis. In the present work, this requirement was met by performing the linear deposition of reagents via the pen-plotting approach. The developed distance-based μPADs fabricated by linear homogenous deposition of a Morin solution over the straight channels, were successfully

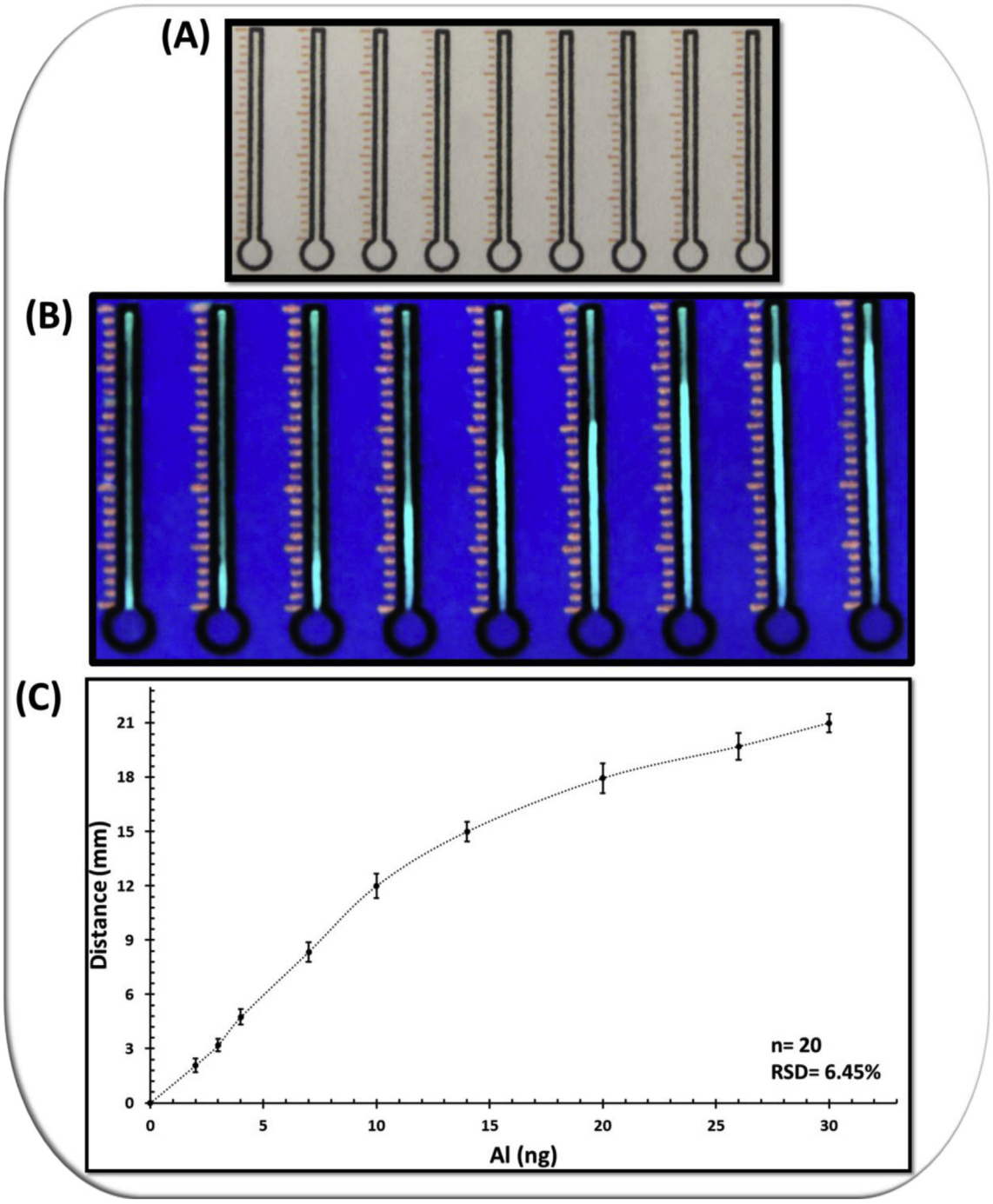

Fig. 4. Distance-based determination of aluminium. (A) Photograph of distance-based μPADs at the end of analysis after pipetting 4 μL of Al standard solutions. No color change or distance signal is observable. (B) Photograph of distance-based μPADs after placing them in the UV viewing cabinet and exposing to 254 nm UV illumination. Contrast and brightness are modified for better observation. (C) Response curve of different concentrations of Al (2–30 ng) to the distance-based μPADs. Markers reflect the average of 20 repeated measurements. The error bars represent the standard deviations from the average values. (For interpretation of the references to color in this figure legend, the reader is referred to the Web version of this article.)

applied for instrument-free quantification of aluminum in water samples. According to the Australian and New Zealand guidelines for fresh and marine water quality, the concentration of Al in irrigation waters should not be more than 5 mg/L (long-term use) or 20 mg/L (short-term use) [34]. In this work, distance-based determination of standard solutions of Al was investigated in the range of 2–30 ng (0.5–7.5 mg/L) and the calibration curve was obtained from the measured distance signals. For the detection of Al(III), the μPADs were exposed to UV light ($\lambda_{max} = 254$ nm) for observation of the fluorescent emission from Morin-Al complex along the channels. The shortest visible length (average = 2.08 ± 0.38 mm) correlated to a sample containing 2 ng of Al, which was then considered as the detection limit (mass detection limit). The actual photograph of μPADs after loading 4 μL of standard Al(III) solutions with various concentrations into the sample inlets are depicted in Fig. 4, along with the corresponding response curves. The standard deviations

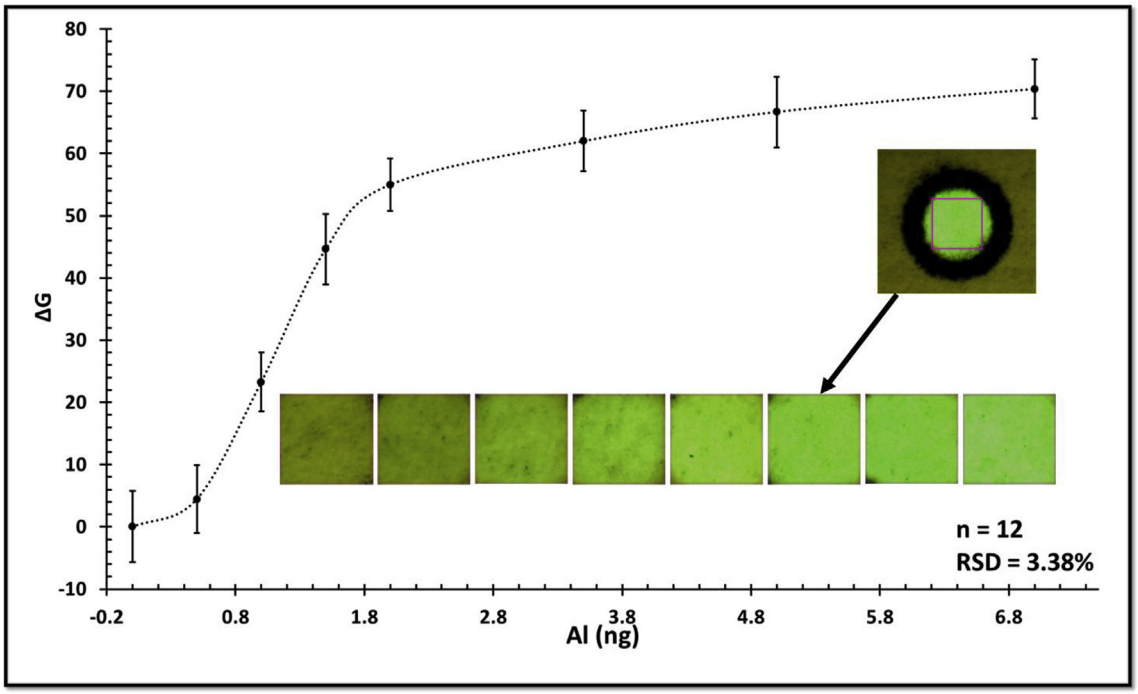

Fig. 5. Color intensity based determination of aluminium. Graph represents the calibration curve associated with Al analysis (1–7 ng) obtained from recorded green intensities (using a fluorescence microscope) at the detection zone of the μPADs. The markers and error bars reflect the average and standard deviations of 12 measurements. Inset: photographs of detection areas of paper after loading with various concentration of Al. (For interpretation of the references to color in this figure legend, the reader is referred to the Web version of this article.)

and error bars in the corresponding graph, represent excellent reproducibility (average RSD = 6.45%, n = 20) of analysis, which indirectly confirms the reliability of the pen-plotting approach for linear deposition of reagents.

The effect of possible co-existing interfering metal ions on the determination of Al was investigated by applying water samples containing Al (2.5 ppm) and different metal ions (Na(I), K(I), Pb(II), Ni(II), Zn(II), Mg(II), Mn(II), Ca(II), Co(II), Cd(II), Cr(II), Fe(II), and Hg(II)) with Al:metal ratio of 1:1. The formation of fluorescent Morin-metal (e.g. Al, Ca, Mg, Be, etc.) complexes is pH dependent and in the specified pH here (pH = 4) is highly selective for Al. In addition, the acetate used in the buffer composition can also function as a masking agent preventing many metal interferences. However, the major interference concern is Fe (III), which would interfere by quenching the fluorescent signal to some extent. The presence of the metal ions did not have a significant impact on the distance signal; however, Fe(III) in Al:metal ratio of more than 1:0.5 caused some interference in the form of fluorescence quenching, which mostly affected the intensity of the formed color band rather than the distance signal. By depositing a mixture of hydroxylamine hydrochloride to reduce Fe(III) to Fe(II), and 1,10-phenanthroline as a masking agent for Fe(II) in the sample zone prior to analysis, an Al:Fe(III) ratio of more than 1:1 could be tolerated.

Real water samples were collected (Ringarooma, Tasmania, Australia), filtered, and spiked with a known concentration (2.5 ppm) of standard Al solution and then analyzed both with the distance-based μPADs and atomic absorption spectroscopy (AAS). Results indicated a good agreement (within 10% error) between these two techniques (Table S-1). The non-spiked water samples did not generate any distance signal on the μPADs indicating normal levels of the target metal in the water sample. This was further confirmed by AAS analysis which showed Al at trace levels and below the detection limit of the distance-based μPADs.

3.3.2. Color intensity based measurement

Circular deposition was also utilized for the determination of Al based on traditional color intensity measurements by deposition of the fluorescent reagent in the well-shaped (circular) μPADs (Movie S-1). The μPADs were loaded with 2 μL of standard solutions of Al with various concentrations and then were allowed to dry (10 min) under ambient conditions. The color intensity based determination was investigated in the range of 0.5–7 ng (0.25–3.5 mg/L) of Al and the calibration curve was obtained for different intensities of green fluorescence emission (G) recorded by fluorescence microscope (Supporting Information). The signals were plotted as ΔG (G_{Sample} - G_{Blank}) versus Al concentrations (Fig. 5). The mass limit of detection (LOD) was calculated to be 0.83 ng of Al, based on three times the standard deviation (3SD) of the signal (green intensity) of the blank. Above 7 ng of Al, the paper surface was saturated with fluorescence emission and no additional increase in green intensity could be measured.

Similar to the distance-based measurements, here the average RSD representing the reproducibility of all tests was 3.38% (n = 12) which indicates the reliability of the pen-plotting approach for circular deposition of reagents as well as for linear deposition. The traditional μPADs present a slightly lower detection limit of Al; however, the distance-based μPADs eliminate the need for external detectors and also enable a much wider dynamic range since detection in traditional μPADs faces color saturation at much lower concentrations compared to distance-based μPADs. A detailed comparison between traditional and distance-based μPADs for determination of Al is shown in Table S2 in the Supporting Information.

4. Conclusions

This study characterizes in detail the pen-plotting approach and

documents it as a versatile, rapid, reproducible, and high-throughput method for deposition of chemical reagents on paper substrates for the development of μPADs. An accurate gravimetric method is introduced which can be readily used in order to determine the volume of deposited reagents and overcome the existing uncertainty in this regard. The versatility of this approach is further illustrated by demonstrating the reagent deposition in both linear and circular forms which can be later implemented in the fabrication of μPADs with a variety of designs and applications.

Traditional color intensity based μPADs utilized circular deposition, and distance-based μPADs utilized linear deposition of fluorescent reagent by pen-plotting for the determination of Al(III) in natural waters. The distance-based μPADs exhibited a much wider dynamic range since detection in traditional μPADs faces color saturation at much lower concentrations. The low RSD values for all the measured parameters obtained from these μPADs indicate the reliability of this approach for reproducible deposition of reagents on μPADs of different designs and sizes. The controlled and reproducible nanolitre scale deposition of chemical inks along with good control over the size and shape of the plotted features may stimulate novel applications even in other research areas demanding localized delivery of chemical reagents.

Acknowledgements

MM gratefully acknowledges the Australian Research Council Future Fellowship (FT120100559). This work was supported by the ESF under the project CZ.02.2.69/0.0/0.0/18_050/0008462.

Appendix A. Supplementary data

Supplementary data related to this article can be found at https://doi.org/10.1016/j.aca.2018.09.006.

References

[1] D.M. Cate, J.A. Adkins, J. Mettakoonpitak, C.S. Henry, Recent developments in paper-based microfluidic devices, Anal. Chem. 87 (2015) 19–41.
[2] Y. Yang, E. Noviana, M.P. Nguyen, B.J. Geiss, D.S. Dandy, C.S. Henry, Paper-based microfluidic devices: emerging Ttemes and applications, Anal. Chem. 89 (2017) 71–91.
[3] M.M. Gong, D. Sinton, Turning the page: advancing paper-based microfluidics for broad diagnostic application, Chem. Rev. 117 (2017) 8447–8480.
[4] K. Yamada, H. Shibata, K. Suzuki, D. Citterio, Toward practical application of paper-based microfluidics for medical diagnostics: state-of-the-art and challenges, Lab a Chip 17 (2017) 1206–1249.
[5] S. Ahmed, M.P.N. Bui, A. Abbas, Paper-based chemical and biological sensors: engineering aspects, Biosens. Bioelectron. 77 (2016) 249–263.
[6] Y. He, Y. Wu, J.Z. Fu, W.B. Wu, Fabrication of paper-based microfluidic analysis devices: a review, RSC Adv. 5 (2015) 78109–78127.
[7] X. Jiang, Z.H. Fan, Fabrication and operation of paper-based analytical devices, Annu. Rev. Anal. Chem. 9 (2016) 203–222.
[8] Y. Xia, J. Si, Z. Li, Fabrication techniques for microfluidic paper-based analytical devices and their applications for biological testing: a review, Biosens. Bioelectron. 77 (2016) 774–789.
[9] D.M. Cate, W. Dungchai, J.C. Cunningham, J. Volckens, C.S. Henry, Simple, distance-based measurement for paper analytical devices, Lab on a Chip - Miniaturisation for Chemistry and Biology 13 (2013) 2397–2404.
[10] Tian, J. Li, Y. Song, L. Zhou, Z. Zhu, C.J. Yang, Distance-based microfluidic quantitative detection methods for point-of-care testing, Lab a Chip 16 (2016) 1139–1151.
[11] X. Wei, T. Tian, S. Jia, Z. Zhu, Y. Ma, J. Sun, Z. Lin, C.J. Yang, Microfluidic distance readout sweet hydrogel integrated paper-based analytical device (μDiSH-PAD) for visual quantitative point-of-care testing, Anal. Chem. 88 (2016) 2345–2352.
[12] M. Srisa-Art, K.E. Boehle, B.J. Geiss, C.S. Henry, Highly sensitive detection of Salmonella typhimurium using a colorimetric paper-based analytical device coupled with immunomagnetic separation, Anal. Chem. 90 (2017) 1035–1043.
[13] T. Tian, Y. An, Y. Wu, Y. Song, Z. Zhu, C. Yang, Integrated distance-based origami paper analytical device for one-step visualized analysis, ACS Appl. Mater. Interfaces 9 (2017) 30480–30487.
[14] R. Pratiwi, M.P. Nguyen, S. Ibrahim, N. Yoshioka, C.S. Henry, D.H. Tjahjono, A selective distance-based paper analytical device for copper (II) determination using a porphyrin derivative, Talanta 174 (2017) 493–499.
[15] N. Komuro, S. Takaki, K. Suzuki, D. Citterio, Inkjet printed (bio)chemical sensing devices, Anal. Bioanal. Chem. 405 (2013) 5785–5805.
[16] B. Creran, X. Li, B. Duncan, C.S. Kim, D.F. Moyano, V.M. Rotello, Detection of bacteria using inkjet-printed enzymatic test strips, ACS Appl. Mater. Interfaces 6 (2014) 19525–19530.
[17] K. Yamada, T.G. Henares, K. Suzuki, D. Citterio, Paper-based inkjet-printed microfluidic analytical devices, Angew. Chem. Int. Ed. 54 (2015) 5294–5310.
[18] A. Apilux, Y. Ukita, M. Chikae, O. Chailapakul, Y. Takamura, Development of automated paper-based devices for sequential multistep sandwich enzyme-linked immunosorbent assays using inkjet printing, Lab on a Chip - Miniaturisation for Chemistry and Biology 13 (2013) 126–135.
[19] J. Lessing, A.C. Glavan, S.B. Walker, C. Keplinger, J.A. Lewis, G.M. Whitesides, Inkjet printing of conductive inks with high lateral resolution on omniphobic “RF paper” for paper-based electronics and MEMS, Adv. Mater. 26 (2014) 4677–4682.
[20] T.G. Henares, K. Yamada, S. Takaki, K. Suzuki, D. Citterio, “Drop-slip” bulk sample flow on fully inkjet-printed microfluidic paper-based analytical device, Sensor. Actuator. B Chem. 244 (2017) 1129–1137.
[21] C. Dixon, J. Lamanna, A.R. Wheeler, Printed microfluidics, Adv. Funct. Mater. 27 (2017).
[22] N. Ruecha, O. Chailapakul, K. Suzuki, D. Citterio, Fully inkjet-printed paper-based potentiometric ion-sensing devices, Anal. Chem. 89 (2017) 10608–10616.
[23] N. Nuchtavorn, M. Macka, A novel highly flexible, simple, rapid and low-cost fabrication tool for paper-based microfluidic devices (μPADs) using technical drawing pens and in-house formulated aqueous inks, Anal. Chim. Acta 919 (2016) 70–77.
[24] M. Rahbar, P.N. Nesterenko, B. Paull, M. Macka, Geometrical alignment of multiple fabrication steps for rapid prototyping of microfluidic paper-based analytical devices, Anal. Chem. 89 (2017) 11918–11923.
[25] K.L. Cheng, K. Ueno, T. Imamura, CRC Handbook of Organic Analytical Reagents, CRC press, 1992.
[26] J. Tria, E.C. Butler, P.R. Haddad, A.R. Bowie, Determination of aluminum in natural water samples, Anal. Chim. Acta 588 (2007) 153–165.
[27] M.J. Ahmed, J. Hossan, Spectrophotometric determination of aluminum by morin, Talanta 42 (1995) 1135–1142.
[28] H.-z. Lian, Y.-f. Kang, S.-p. Bi, A. Yasin, D.-l. Shao, Y.-j. Chen, L.-m. Dai, L.-c. Tian, Morin applied in speciation of aluminum in natural waters and biological samples by reversed-phase high-performance liquid chromatography with fluorescence detection, Anal. Bioanal. Chem. 376 (2003) 542–548.
[29] J. Credou, R. Faddoul, T. Berthelot, Photo-assisted inkjet printing of antibodies onto cellulose for the eco2-friendly preparation of immunoassay membranes, RSC Adv. 5 (2015) 29786–29798 (T).
[30] D.M. Cate, S.D. Noblitt, J. Volckens, C.S. Henry, Multiplexed paper analytical device for quantification of metals using distance-based detection, Lab on a Chip - Miniaturisation for Chemistry and Biology 15 (2015) 2808–2818.
[31] K. Yamada, T.G. Henares, K. Suzuki, D. Citterio, Distance-Based Tear Lactoferrin Assay on microfluidic paper device using interfacial interactions on surface-modified cellulose, ACS Appl. Mater. Interfaces 7 (2015) 24864–24875.
[32] B. Sarkar, Heavy Metals in the Environment, CRC Press, 2002.
[33] E. Underwood, Trace Elements in Human and Animal Nutrition, Elsevier, 2012.
[34] ANZECC, ARMCANZ, (Australian and New Zealand Environmental and Conservation Council, Agriculture and Resource Management Council of Australia and New Zealand, Canberra) Australian and New Zealand Guidelines for Fresh and Marine Water Quality. No. 4, vol. 3, 2000 (Chapter 9).